GEOLOGICAL SURVEY OF CANADA
COMMISSION GEOLOGIQUE DU CANADA

Open File 2934

WESTERN CANADA SEDIMENTARY BASIN BOREHOLE IMAGERY ANALYSIS PROJECT: A SUMMARY OF MOBIL PHILLIPS SUKUNKA d-70-I/93-P-4

R.E. McCallum[1] and J.S. Bell[2]

[1] R.E.M. Consulting, 1447 19 Ave. S.W., Calgary, Alberta T2T 0J1

[2] Institute of Sedimentary and Petroleum Geology, Geological Survey of Canada
3303 33 Street N.W., Calgary, Alberta T2L 2A7

SEPTEMBER 1994

Western Canada Sedimentary Basin Borehole Imagery Analysis Project: A Summary of Mobil Phillips Sukunka D-70-I/93-P-4

Well Name: Mobil Philips Sukunka d-70-I/93-P-4

Operator: Mobil Oil

Location: latitude 55° 13' 24.19" N
longitude 121° 37' 01.85" W
(see figure 1)

Rig Release Date: 1991-11-23

Imagery Log/Interval Logged: FMS 2550.0 - 3161.5 m
FMI 3167.0 - 3592.0 m

Only FMS examined

Well Trajectory: Semi-vertical, deviated

Drill Bit Size: 14.9 inches over the interval logged

Formations Logged:

Jurassic Nikanassin	629.3 m
Jurassic Passage Beds	2780.0 m
Jurassic Fernie Shale	2890.0 m
Jurassic Glauconite marker	3163.7 m

Lithologies: The upper part of the section logged consists of the sandstones and siltstones of the Jurassic Nikanassin Formation. The remainder of the interval is comprised largely of shales of the Jurassic Passage Beds Formation and Fernie Shale Group.

Core Intervals: None that correspond to FMS imaged intervals.

Structural Setting: Foothills thrust belt

Regional Stress trajectories: The nearest wells with stress orientation data are Canadian Resources QUINTANA ADSETT b-14-G/94-J-2 and Coseka et al NEPTUNE d-84-G/94-J-8 each with S_{Hmin} directions of 152.3° N and 157° N respectively (Bell et al, in press).

Description of Images:

Drilling Induced Fractures:

Vertical Fractures: Over 150 vertical induced fractures were observed in the interval and examples are given in figures 3,4,5,7 and 8. The fractures are characterized by thin,

continuous, dark (conductive) traces appearing 180° apart on the FMS microresistivity images. The interpretive software program FLIP, converts digital microresistivity contrasts into brown-yellow tones (dark colors indicate high conductivity whereas light colors indicate low conductivity, Bourke et al 1989) and applies a sinusoidal curve to arrive at a true dip angle and dip azimuth. Vertical and horizontal scales of the images are 1:5 to allow as realistic a presentation as possible.

Chatter Fractures: Short, discontinuous, dark (conductive) traces on the FMS log that trend obliquely to borehole trajectory and occur in groups in an en echelon, steplike fashion are interpreted as drilling induced chatter fractures. These appear on opposite sides of the borehole wall 180° to each other. Figure 6 is an example of chatter fractures observed in Sukunka D-70-I/93-P-4. Vertical and horizontal scales of the images are 1:5 to allow as realistic a presentation as possible. On the variable-intensity FMS images, dark colors indicate high conductivity whereas light colors indicate low conductivity.

Borehole Breakouts:

Borehole breakouts are measured by the four oriented arms of the FMS calipers to determine the profile of the wellbore (Plumb and Hickman, 1985). In the presence of anisotropic horizontal stresses borehole collapse may occur on opposite sides of the wellbore at the azimuths of the minimum horizontal stress directions (S_{Hmin}). The calipers will indicate a corresponding long axis where spalling has occurred and a perpendicular short axis near bit size. When the FMS tool is raised through a breakout zone, tool rotation will cease if the pads become entrenched within the zone. Frequently the pads themselves will be unable to make firm contact with the borehole wall in the spalled zone and a diffuse, unfocussed image will result. Figures 2,6,9,10 are examples of borehole breakouts observed in Sukunka D-70-I/93-P-4. Vertical and horizontal scales of the images are 1:5 to allow as realistic a presentation as possible. On the variable-intensity FMS images, dark colors indicate high conductivity whereas light colors indicate low conductivity.

Incipient Breakouts: In Sukunka D-70-I/93-P-4 there are no observed instances of incipient borehole breakout.

Results:

Drilling Induced Fractures:

Vertical Fractures: In Mobil Phillips Sukunka D-70-I/93-P-4 extensive vertical induced fractures are observed throughout the interval logged by the FMS tool. On FMS microresistivity images they are characterized by thin, continuous, dark (conductive), linear traces that parallel borehole trajectory, cross-cut bedding, and are open and mud-filled. They occur 180° apart on the images and range in length from 0.5 m to 4 m. Strike azimuths are summarized in figure 11a. The mean strike azimuth from 157 samples is 037.4° N (standard deviation +/- 1.7°) and the mean dip angle is 88.2°.

It is believed that these fractures form as hydraulic fractures in response to pressure

exerted on the undrilled rock by the weight of the drillstem during drilling. Alternatively, fracture generation may be the result of the drillpipe acting as a loose fitting piston when it is run into the hole too quickly. This action will cause bottomhole pressures to exceed the parting pressure of the rocks (Dickey, 1986).

Hydraulic fractures propagate within the plane formed by the largest and intermediate principal stresses (S_v and S_{Hmax}) and are extensional. S_v is vertical and thus induced fractures can be used to detect the direction of the maximum horizontal principal stress (S_{Hmax}). As figure 10a illustrates, this would give an S_{Hmax} azimuth of 037.4° N at Sukunka D-70-I/93-P-4.

It is this geometric relationship with respect to the stress regime that is useful in distinquishing induced fractures from naturally occurring ones. Natural fractures need not so align themselves in a direction parallel to S_{Hmax}. In addition, induced fractures parallel borehole trajectory whereas natural ones need not.

Chatter Fractures: Figure 11b summarizes the orientations of over fifty chatter fractures observed in Sukunka D-70-I/93-P-4. Mean strike azimuth for the fracture set is computed as 050° N (standard deviation +/- 4.0°) and the mean dip magnitude is 87.7°. Chatter fractures often appear on opposite sides of the borehole wall and may be stratabound. They are believed to be "drilling enhanced" natural fractures (Heliot et al, 1990) formed when a preexisting natural fracture is opened preferentially in the plane of S_{Hmax} and S_v in response to pressure exerted on the rock formation during drilling. This gives rise to the characteristic en echelon, steplike fashion of chatter fractures.

Borehole Breakouts: A stress regime characterized by anisotropic horizontal stresses acting on the borehole will often result in borehole collapse on opposite sides of the well. Borehole breakouts form when shear fractures develope subparallel to the borehole wall and extend the well in a direction parallel to S_{Hmin}. As these fractures propagate, portions of the borehole wall spall off creating an "ovalized" borehole. These features are excellent indicators of the direction of the minimum horizontal stress orientation S_{Hmin}, although cable torque on the tool may bias results slightly (Parker and Hefferman, 1992). Figure 12 summarizes the orientations of observed borehole breakouts. The mean strike azimuth is 121.7° N with a standard deviation of +/- 1.9°. This indicates a mean S_{Hmin} direction of 121.7° N for Sukunka D-70-I/93-P-4.

Conclusions

In Sukunka D-70-I/93-P-4 FMS microresistivity images indicate a mean S_{Hmax} direction of 037.4° N. This orientation is in agreement with regional trends of S_{Hmax} as summarized in figure 1. The mean S_{Hmin} direction of 121.7° N differs from S_{Hmin} directions derived from oriented caliper logs from nearby wells QUINTANA ADSETT b-14-G/94-J-2 and NEPTUNE d-84-G/94-J-8, each with values of 152.3° N and 157.0° N respectively. Despite these differences there is an approximate agreement with the regional trends (see figure 1).

Fig. 1 Location of Sukunka d-70-I/93-P-4 with respect to the stress regime of the Western Canada Sedimentary Basin.

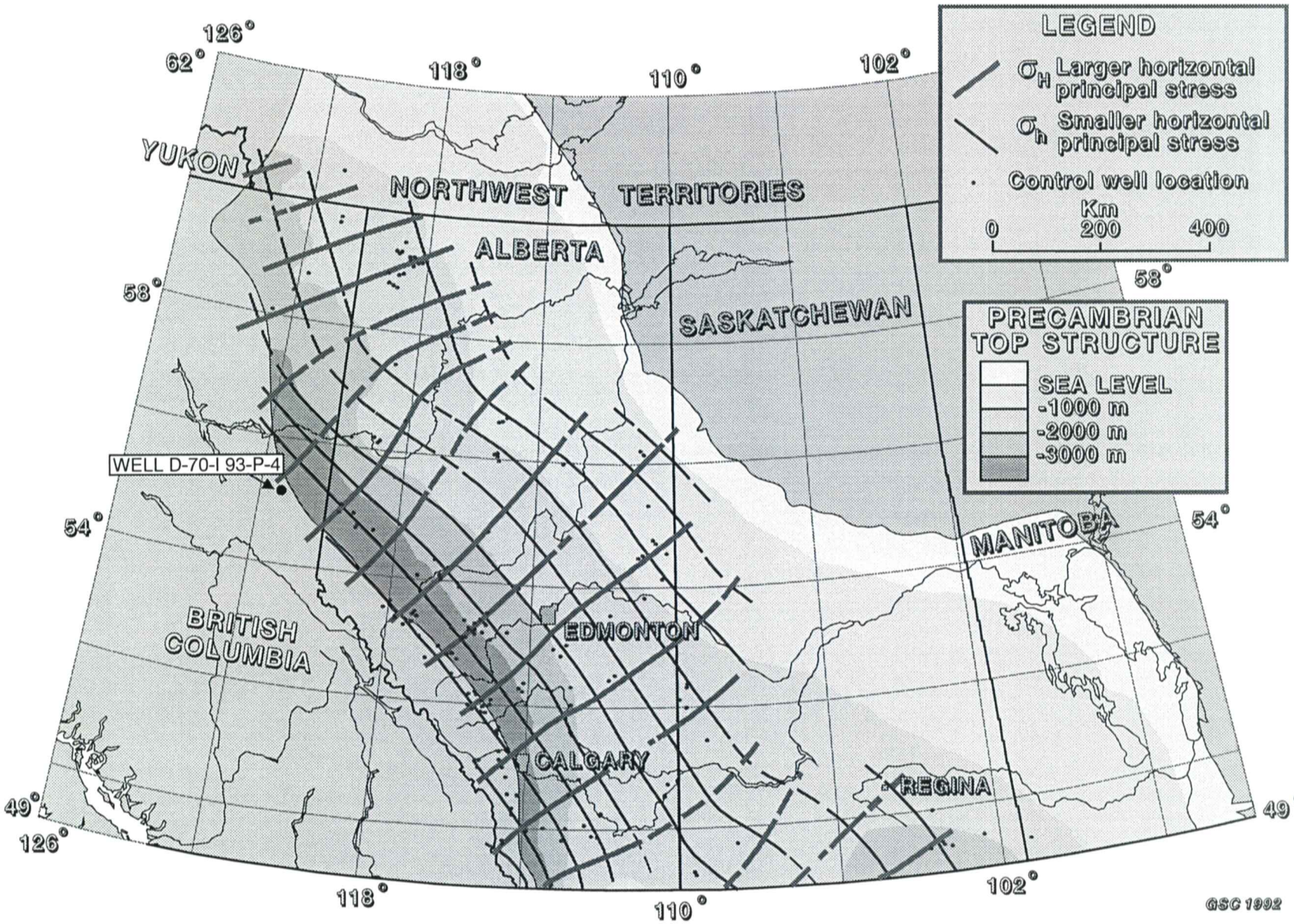

Fig. 1. Location of well D-70-I 93-P-4 with respect to the stress regime of the Western Canada Sedimentary Basin.

Fig. 2 A borehole breakout at the 2552.0 m to 2554.0 m mark within the Nikanassin Formation. The interval consists primarily of sandstones and siltstones. The images on tracks 1 (120°) and 3 (300°) have a diffuse, unfocussed character due to the inability of the tool pads to make firm contact with the caved portion of the borehole wall. Note the extension of the first and third caliper arms. This indicates borehole ovalization in a WNW-ENE direction and a S_{Hmin} direction of 120° N.

Tracks 2 and 4 are at 210° and 30° respectively.

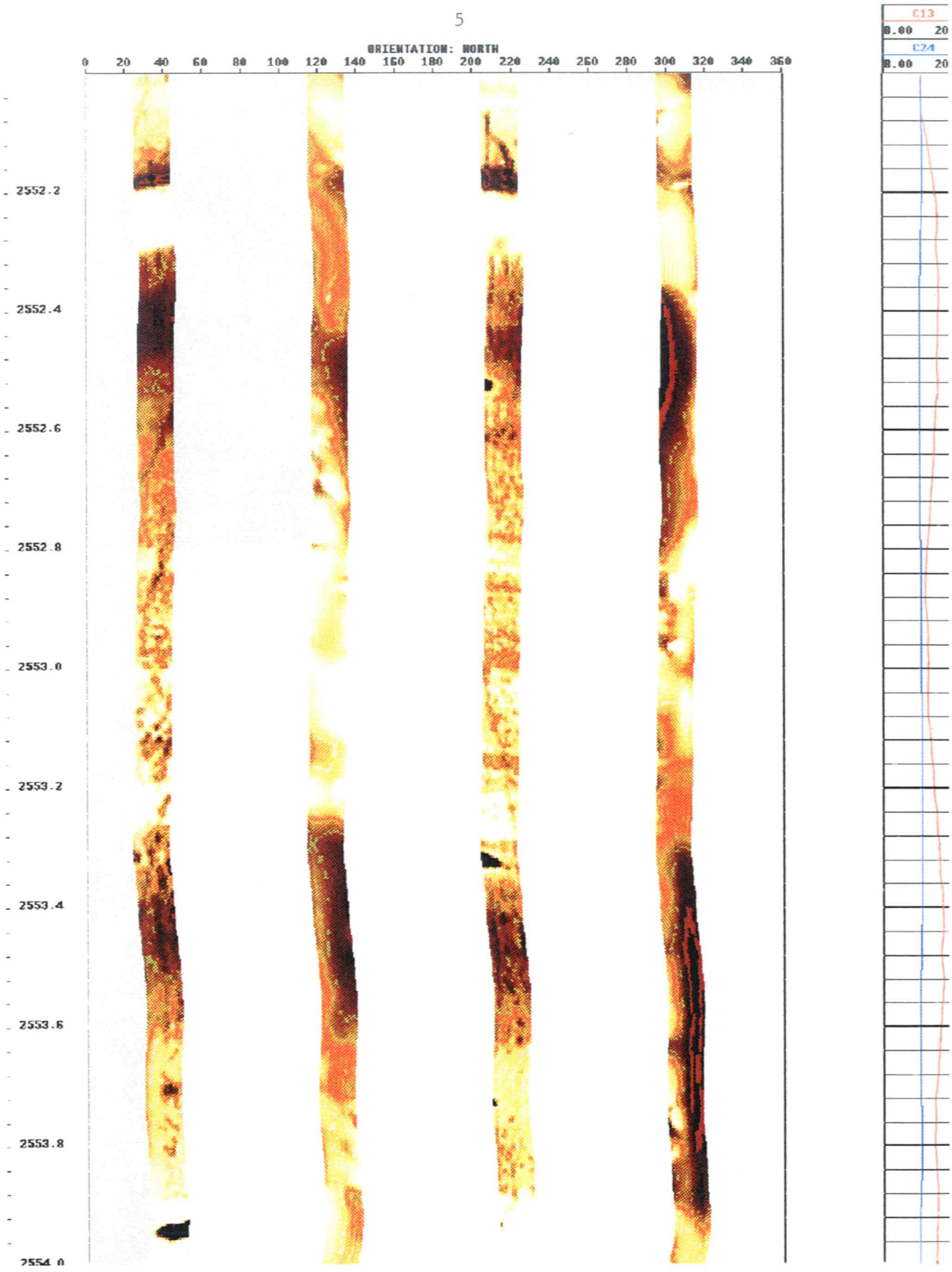
ORIENTATION: NORTH
0 20 40 60 80 100 120 140 160 180 200 220 240 260 280 300 320 340 360
2552.2
2552.4
2552.6
2552.8
2553.0
2553.2
2553.4
2553.6
2553.8
2554.0
C13
0.00 20
C24
0.00 20

Fig 3. A vertical induced fracture and borehole breakout at the 2554.0 to 2556.0 m mark. The fracture, characterized by the thin dark (conductive) trace dips steeply at 88° and strikes 038° (TD 88/308 means a true dip angle of 88° and a dip azimuth of 308°). The images on tracks 1 (130°) and 3 (310°) are diffuse and unfocussed, and the extended arms of calipers 1 and 3 indicate borehole ovalization in a NW-SE direction. This image indicates a S_{Hmax} direction of 038° N and a S_{Hmin} direction of 130° N.

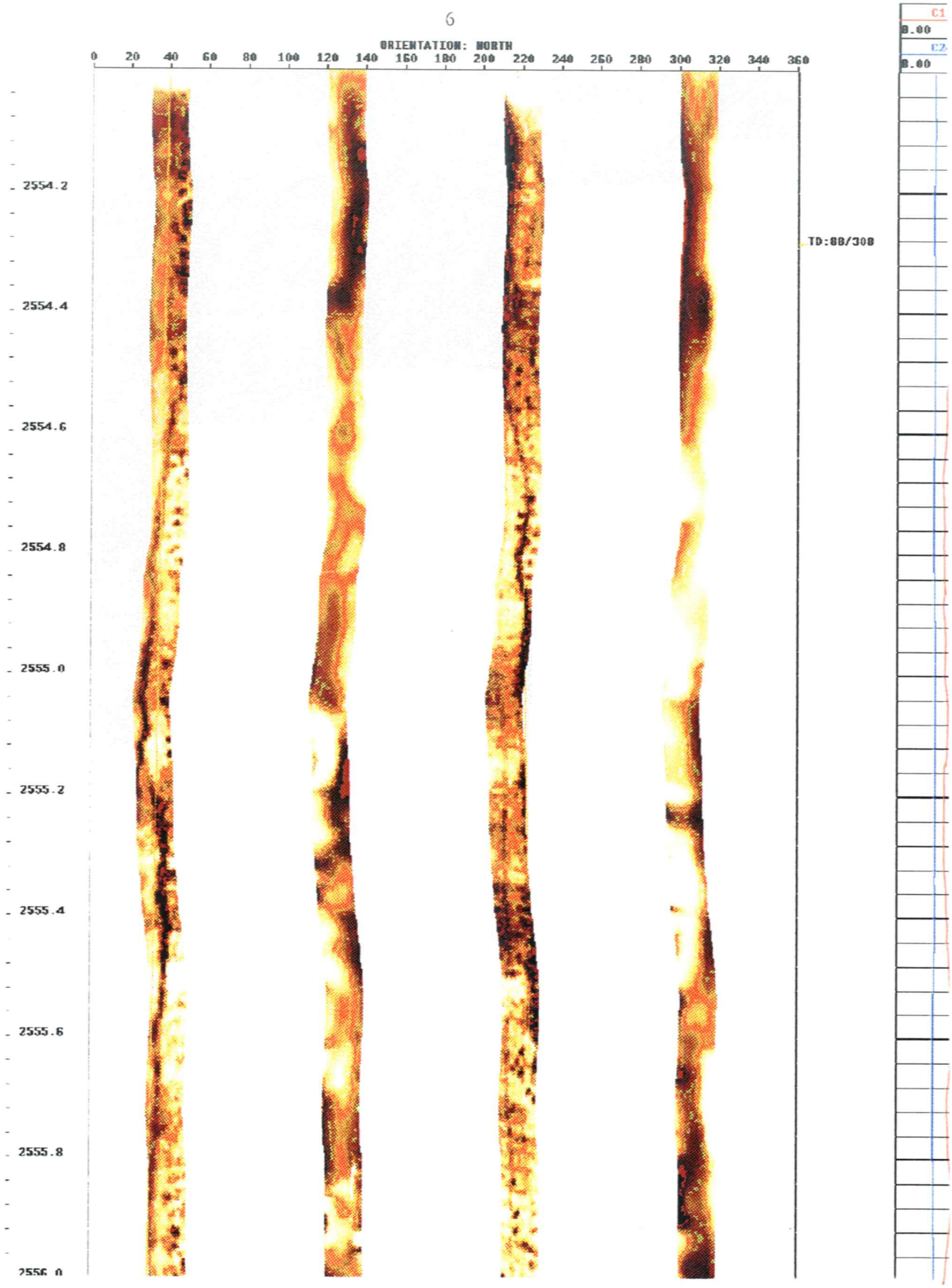
ORIENTATION: NORTH
0 20 40 60 80 100 120 140 160 180 200 220 240 260 280 300 320 340 360
2554.2
2554.4
2554.6
2554.8
2555.0
2555.2
2555.4
2555.6
2555.8
2556.0
TD:88/308
C1
0.00
C2
0.00

Fig. 4 Drilling induced vertical fracture dipping 90° and striking 034° within the Nikanassin Formation. The interval is comprised of sandstone and siltstone. Note the exceptionally clear and continuous trace of the fracture over the 2 m interval in tracks 4 (20°) and 2 (200°). This image indicates a S_{Hmax} direction of 034° N.

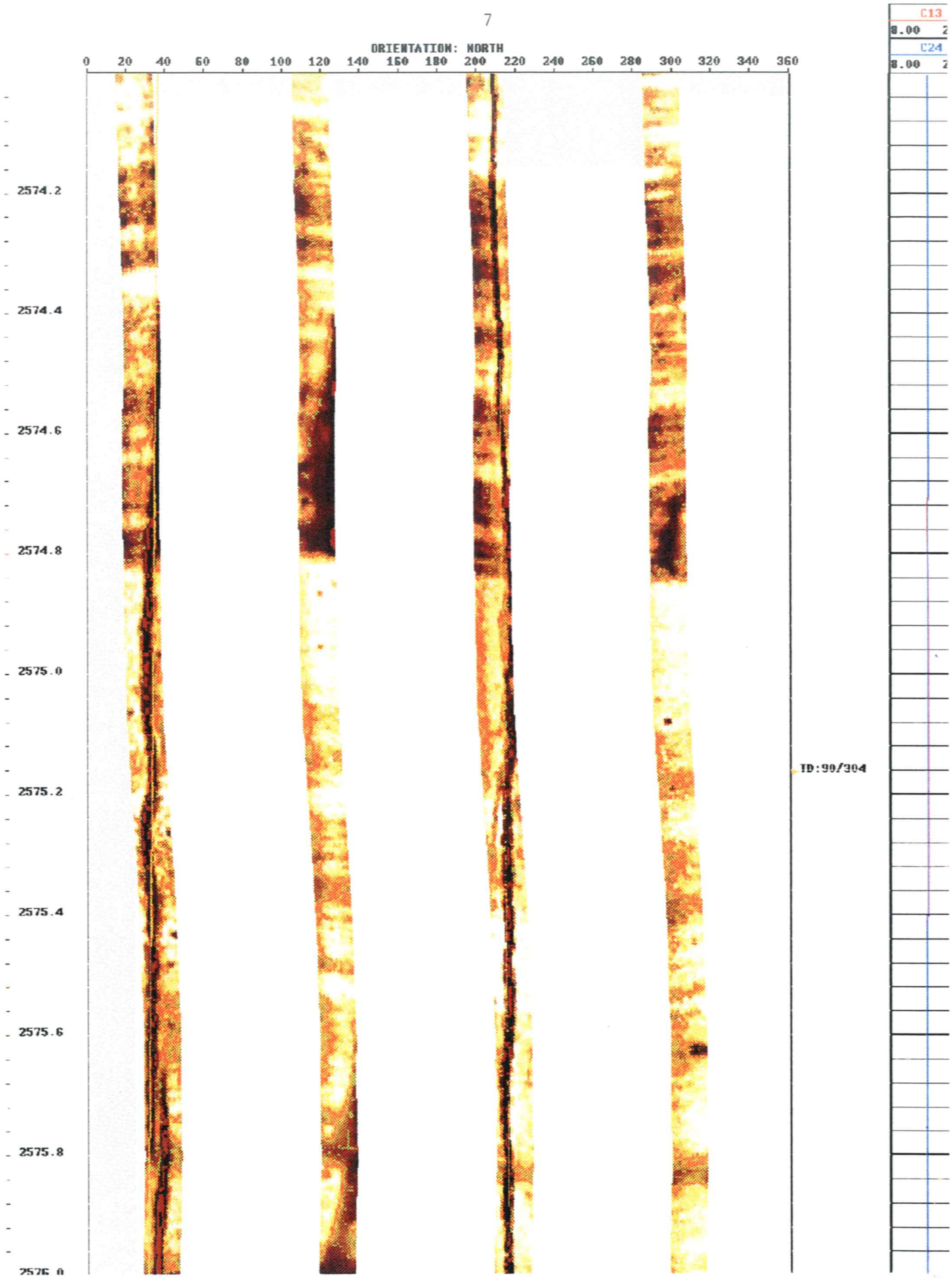
ORIENTATION: NORTH
0 20 40 60 80 100 120 140 160 180 200 220 240 260 280 300 320 340 360
2574.2
2574.4
2574.6
2574.8
2575.0
2575.2
2575.4
2575.6
2575.8
2576.0
ID:90/304
C13
8.00
C24
8.00

Fig. 5 An induced vertical fracture and borehole breakout at the 2582.0 to 2584.0 m mark. The interval consists of sandstones and siltstones of the Nikanassin Formation. The continuous dark (conductive) trace of the open mud-filled fracture on tracks 4 (30°) and 2 (210°) is in contrast with the diffuse unfocussed images of tracks 1 (120°) and 3 (300°). The fracture dips at 89 ° and strikes 038° N. Calipers 1 and 3 are extended indicating borehole ovalization in a NW-SE direction. The image indicates S_{Hmax} at 038° N and S_{Hmin} at 120° N.

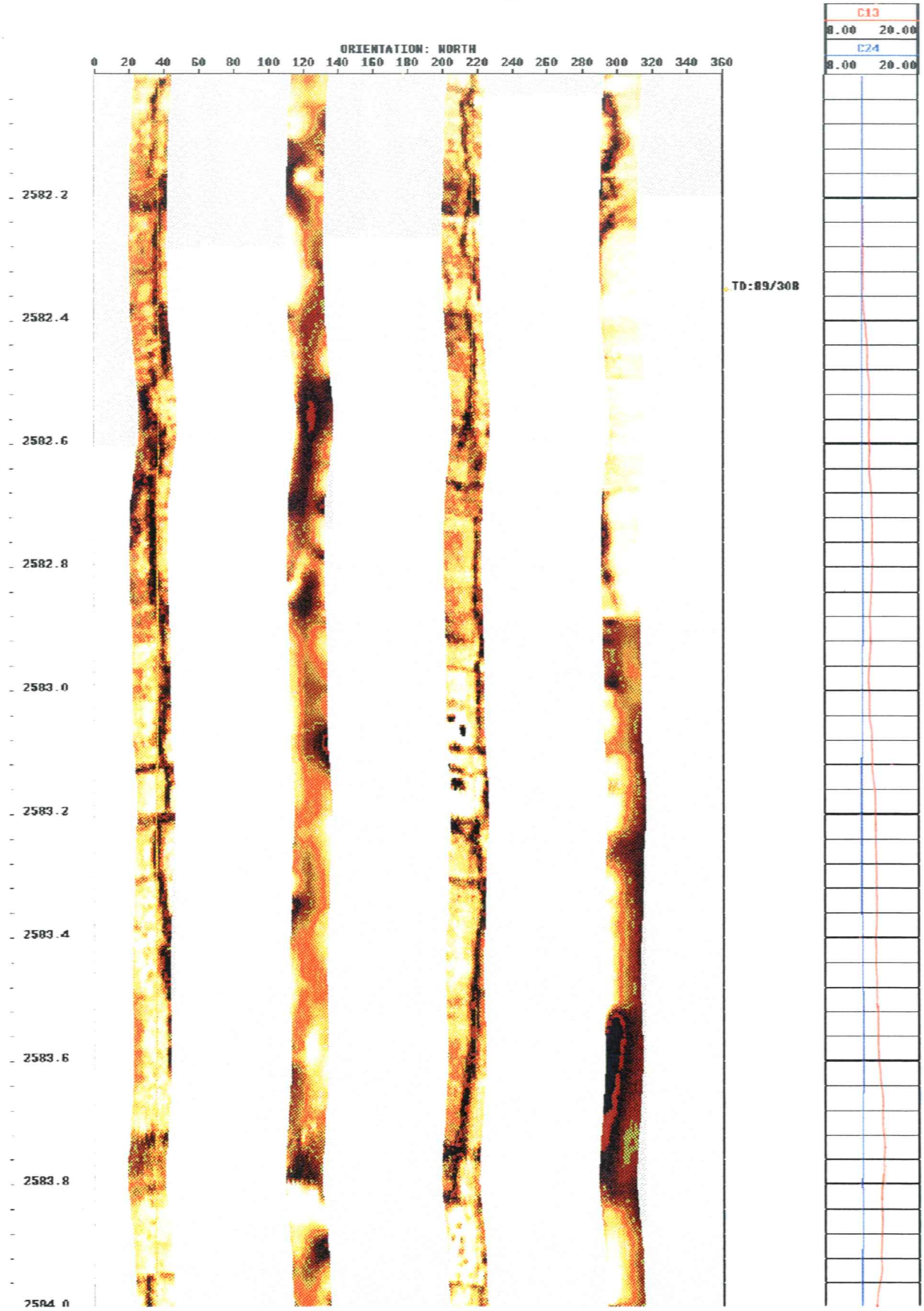
ORIENTATION: NORTH
0 20 40 60 80 100 120 140 160 180 200 220 240 260 280 300 320 340 360
2582.2
2582.4
2582.6
2582.8
2583.0
2583.2
2583.4
2583.6
2583.8
2584.0
TD:89/308
C13
8.00 20.00
C24
8.00 20.00

Fig. 6 Chatter fractures and borehole breakout at 2585.6 to 2587.6 m. The interval consists of sandstones and siltstones of the Nikanassin Formation. Images on tracks 1 and 3 at 120° and 300° display an unfocussed, diffuse character and calipers 1 and 3 widen to a maximum between 2586.2 m and 2586.8 m. Note how tool rotation resumes below this interval at 2586.8 m as the tool pads leave the caved zone. The fractures overlap each other in a slanted, en echelon, step-like fashion. They appear on opposite sides of the borehole 180° apart. Note how the fracture traces on track 4 (030°) at 2587.2 m are bounded by a bedding layer. This illustrates the control of lithology and preexisting discontinuities on induced fracture development.

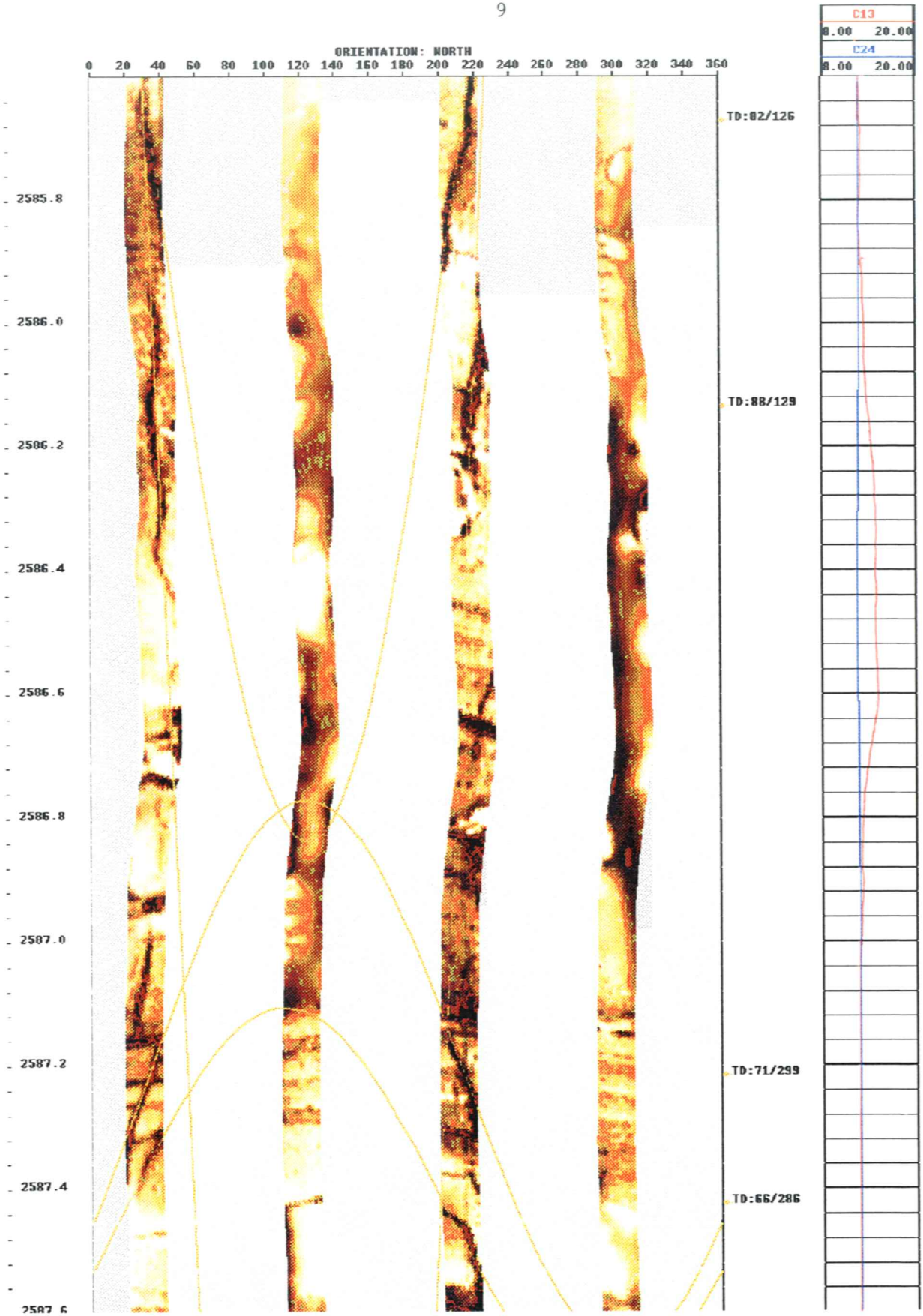
ORIENTATION: NORTH
0 20 40 60 80 100 120 140 160 180 200 220 240 260 280 300 320 340 360
TD:82/126
TD:88/129
TD:71/299
TD:66/286
2585.8
2586.0
2586.2
2586.4
2586.6
2586.8
2587.0
2587.2
2587.4
C13
8.00 20.00
C24
8.00 20.00

Fig. 7 Vertical induced fractures at the 2611.8 to 2614.0 m interval. The interval consists of sandstone and siltstone of the Nikanassin Formation. The fractures, characterized by dark (conductive) traces of medium aperture on tracks 4 and 2 (30° and 210°), dip at 90° and strike 036°. Track 4 (30°) reveals 3 fractures one on top of the other in the narrow azimuth band represented by the track. The middle fracture has a curved lower end at 2613.2 m. This image indicates a S_{Hmax} direction of 036° N.

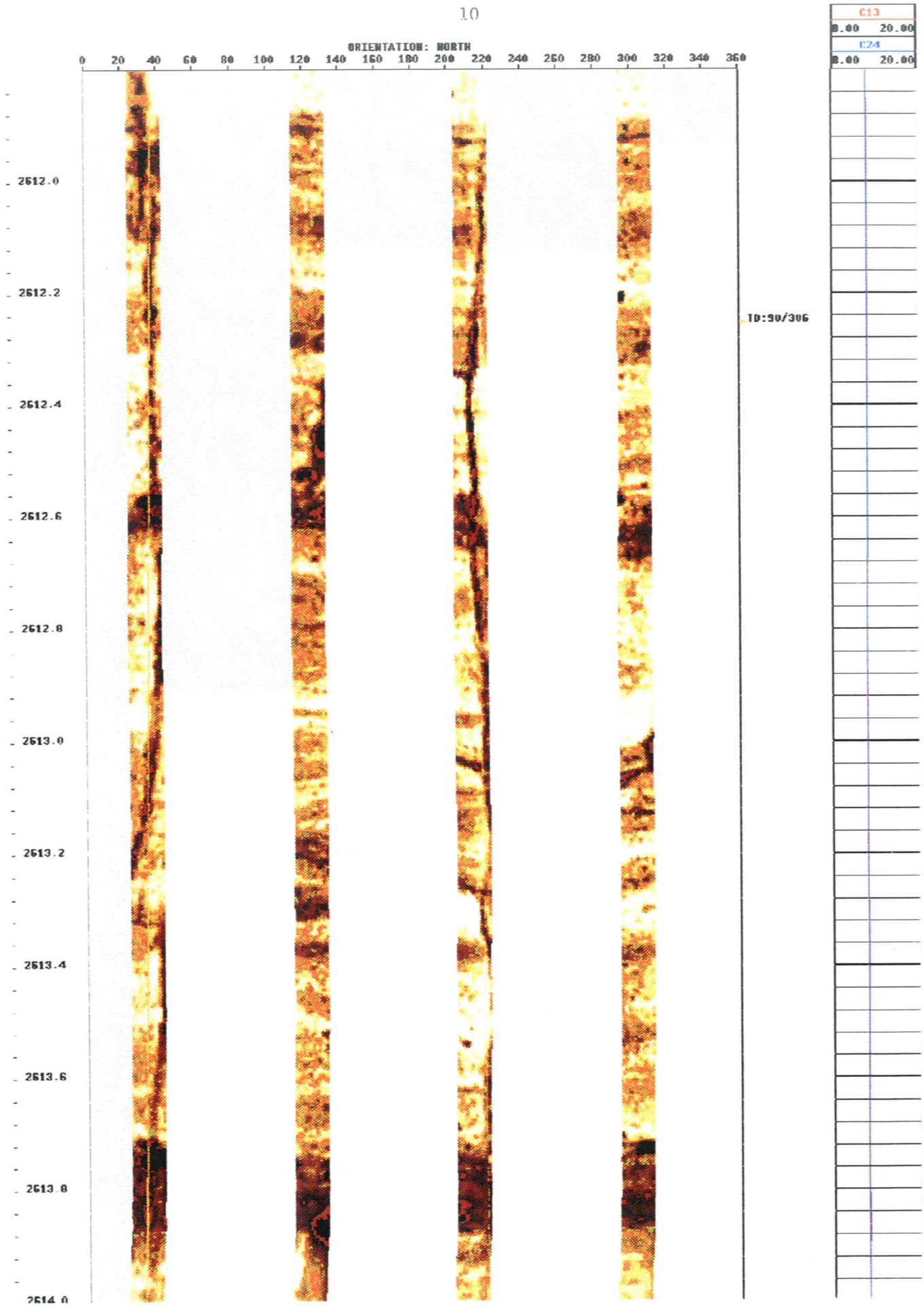
ORIENTATION: NORTH
0 20 40 60 80 100 120 140 160 180 200 220 240 260 280 300 320 340 360
2612.0
2612.2
2612.4
2612.6
2612.8
2613.0
2613.2
2613.4
2613.6
2613.8
2614.0
ID:90/306
C13
0.00 20.00
C24
0.00 20.00

Fig. 8 Three steeply dipping fractures within the 2821.8 m to 2824.0 m interval. The interval lies within the shales of the Passage Beds Formation. The dark (conductive) fracture traces clearly cross-cut bedding and vary in true dip angle from 79° to 85°, and strike in an ENE-WSE direction, indicating a S_{Hmax} direction of approximately 061° N. This image shows how the interpretive software program FLIP, which converts digital microresistivity contrasts into brown-yellow tones (dark colors indicate high conductivity) applies a sinusoidal curve (arbitralily chosen to be yellow) to arrive at a true dip angle and dip azimuth.

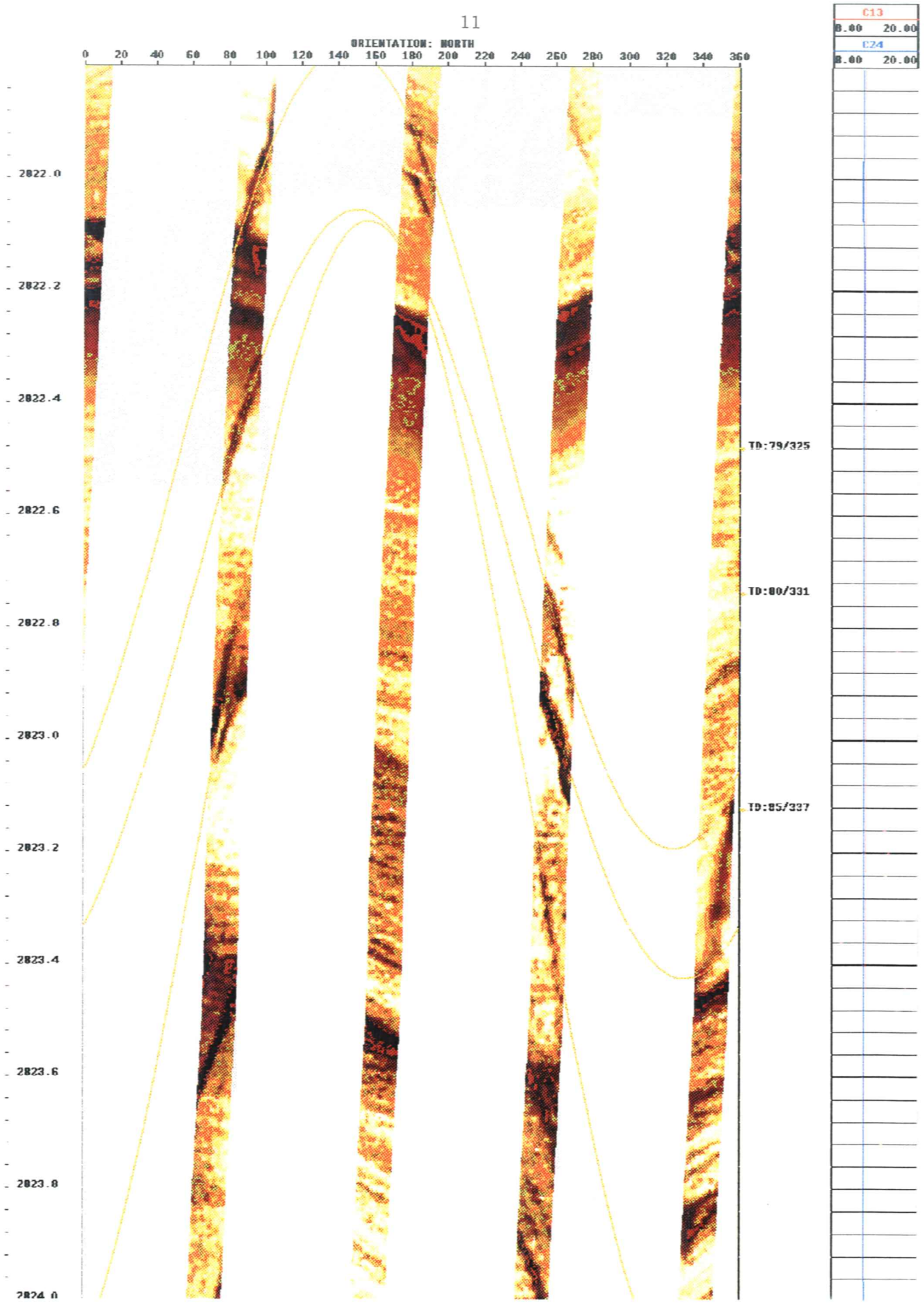
ORIENTATION: NORTH
0 20 40 60 80 100 120 140 160 180 200 220 240 260 280 300 320 340 360
2022.0
2022.2
2022.4
2022.6
2022.8
2023.0
2023.2
2023.4
2023.6
2023.8
2024.0
TD:79/325
TD:80/331
TD:85/337
C13
0.00 20.00
C24
0.00 20.00

Fig. 9 A borehole breakout at the 2969.8 m to 2972.0 m interval. The images in tracks 2 (100°) and 4 (280°) display the unfocussed, diffuse character common to breakouts. Calipers 2 and 4 show maximum extension between 2970.6 m and 2971.4 m, a zone of little or no tool rotation. Borehole ovalization is in an approximate E-W direction indicating a S_{Hmin} direction of 100° N.

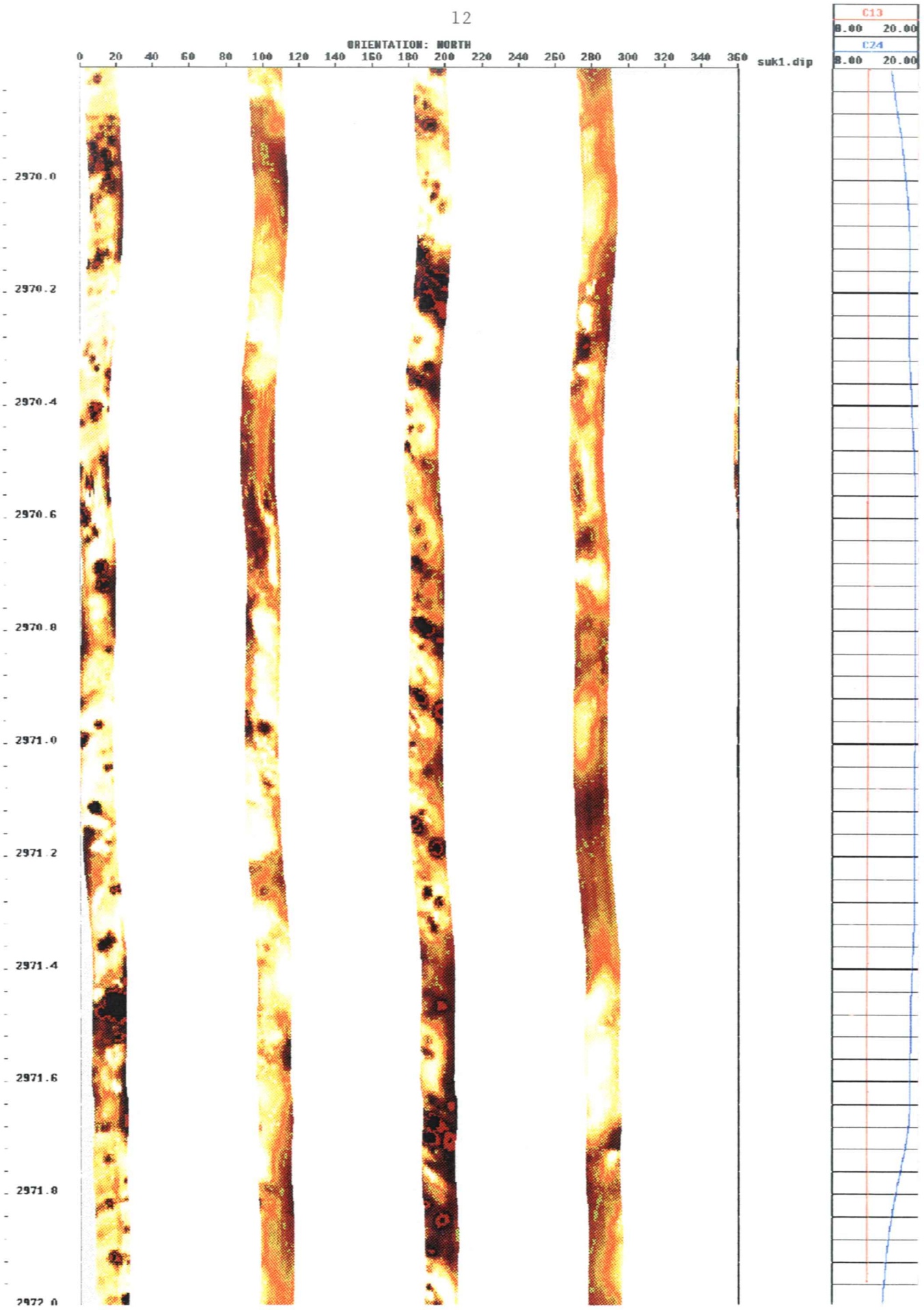
ORIENTATION: NORTH
0 20 40 60 80 100 120 140 160 180 200 220 240 260 280 300 320 340 360
suk1.dip
2970.0
2970.2
2970.4
2970.6
2970.8
2971.0
2971.2
2971.4
2971.6
2971.8
2972.0
C13
0.00 20.00
C24
0.00 20.00

Fig. 10 Zone of extensive borehole collapse at the 3003.6 m to 3005.6 m mark. The interval lies within the Fernie Shale Group. Diffuse, unfocussed images on all tracks as well as significant extension of calipers 2 and 4 suggest ovalization in a ESE-WNW direction and a S_{Hmin} direction of 115° N.

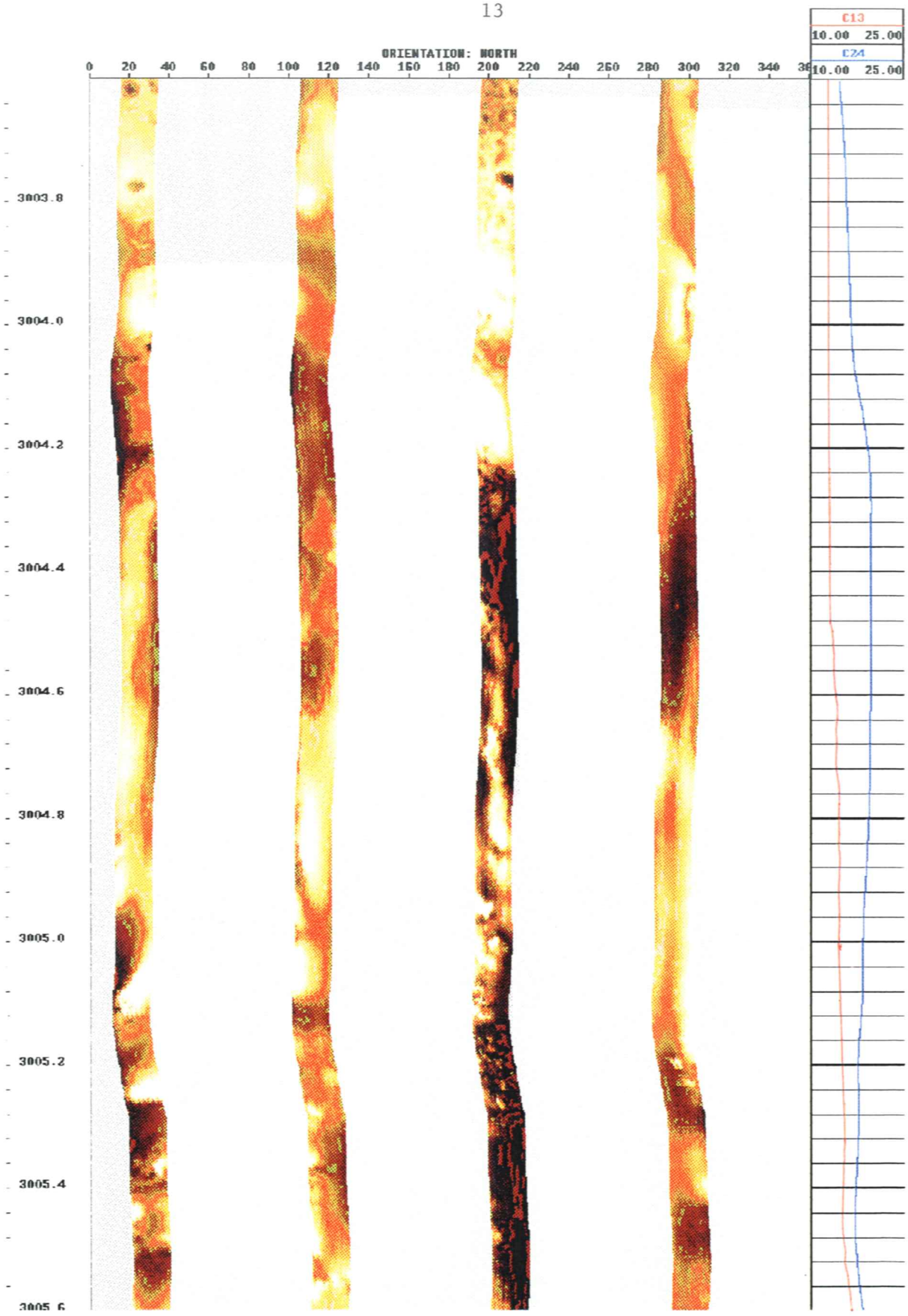
C13
10.00 25.00
C24
10.00 25.00
ORIENTATION: NORTH
0 20 40 60 80 100 120 140 160 180 200 220 240 260 280 300 320 340 360
3003.8
3004.0
3004.2
3004.4
3004.6
3004.8
3005.0
3005.2
3005.4
3005.6

Fig. 11a Strike azimuth plot of vertical fractures in Sukunka D-70-I/93-P-4. Mean strike azimuth for 157 samples is computed as 037.4° N (RMS = 1.7°) with a mean dip magnitude of 88.2°.

Fig. 11b Strike azimuth plot of chatter fractures in Sukunka d-70-i. Mean strike azimuth for 55 samples is computed as 050° N (RMS = 4.0°) with a mean dip magnitude of 87.7°.

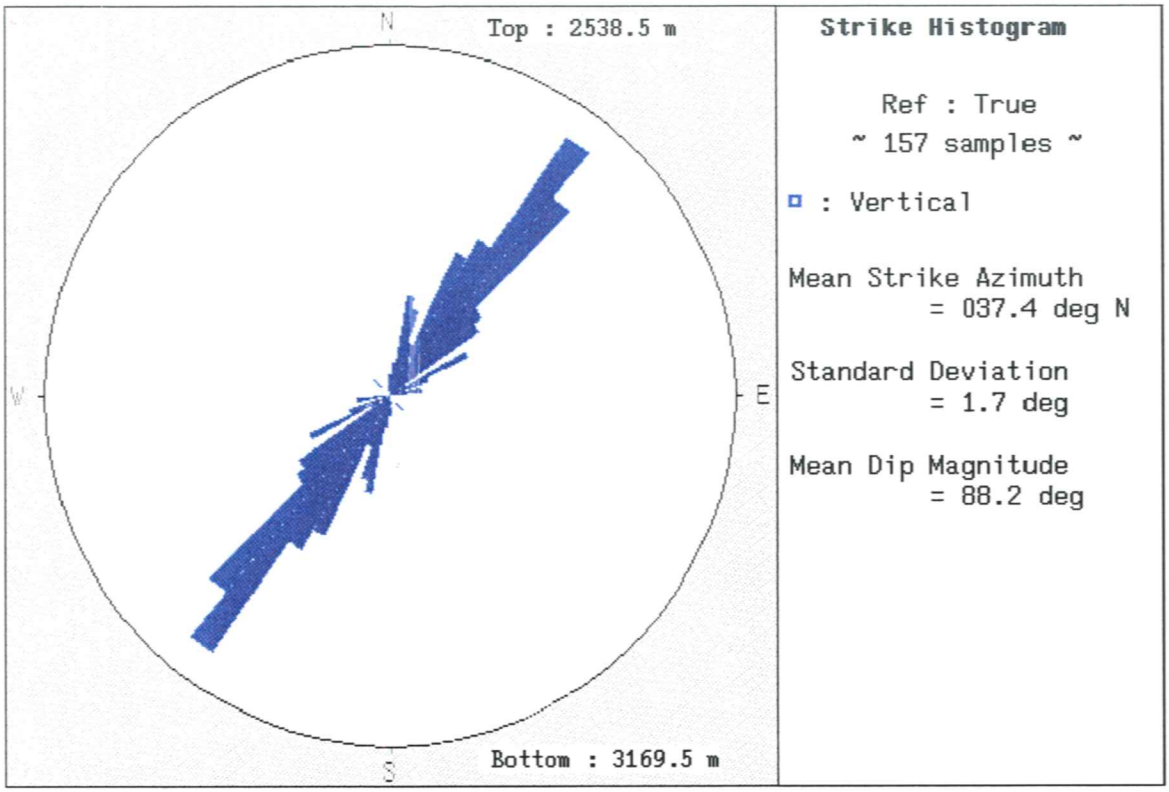
N
Top : 2538.5 m
W
E
S
Bottom : 3169.5 m
Strike Histogram
Ref : True
~ 157 samples ~
: Vertical
Mean Strike Azimuth
= 037.4 deg N
Standard Deviation
= 1.7 deg
Mean Dip Magnitude
= 88.2 deg

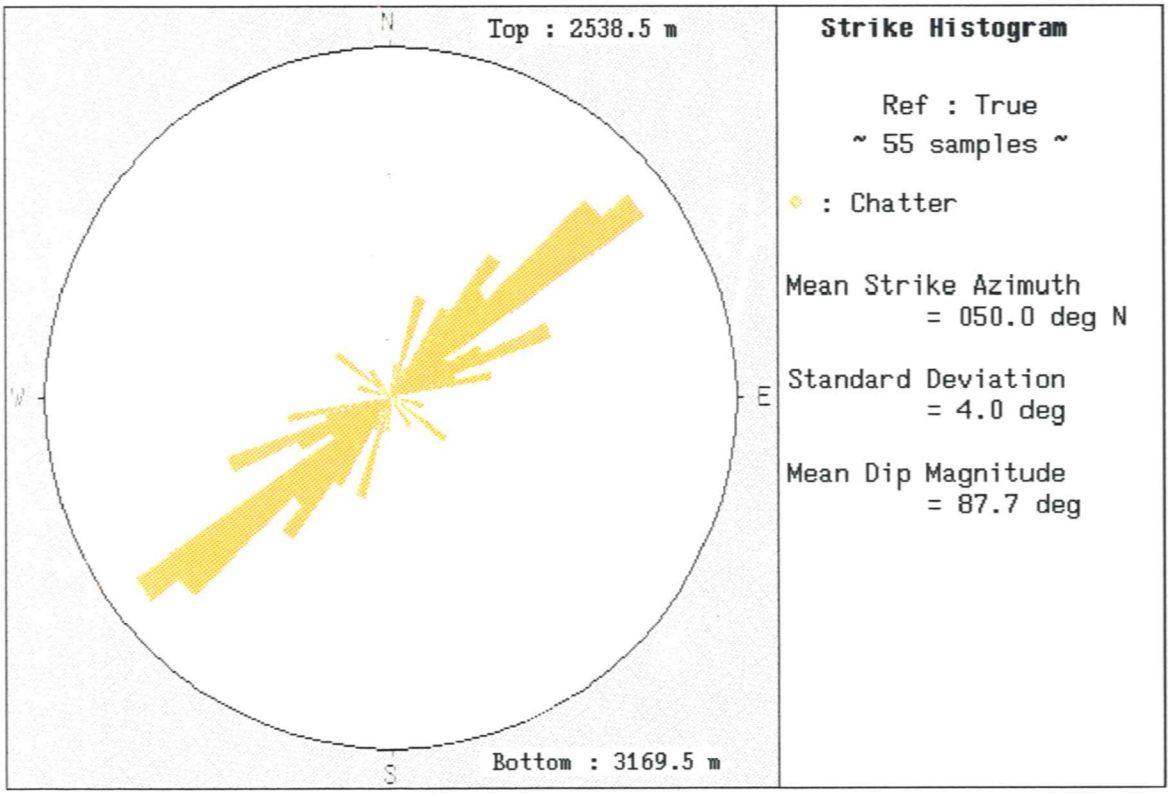
N
Top : 2538.5 m
W
E
S
Bottom : 3169.5 m
Strike Histogram
Ref : True
~ 55 samples ~
: Chatter
Mean Strike Azimuth
= 050.0 deg N
Standard Deviation
= 4.0 deg
Mean Dip Magnitude
= 87.7 deg

Fig. 12 Strike azimuth plot of borehole breakouts in Sukunka D-70-I/93-P-4. Mean strike azimuth for 99 samples is computed as 121.7° N (RMS = 1.9°).

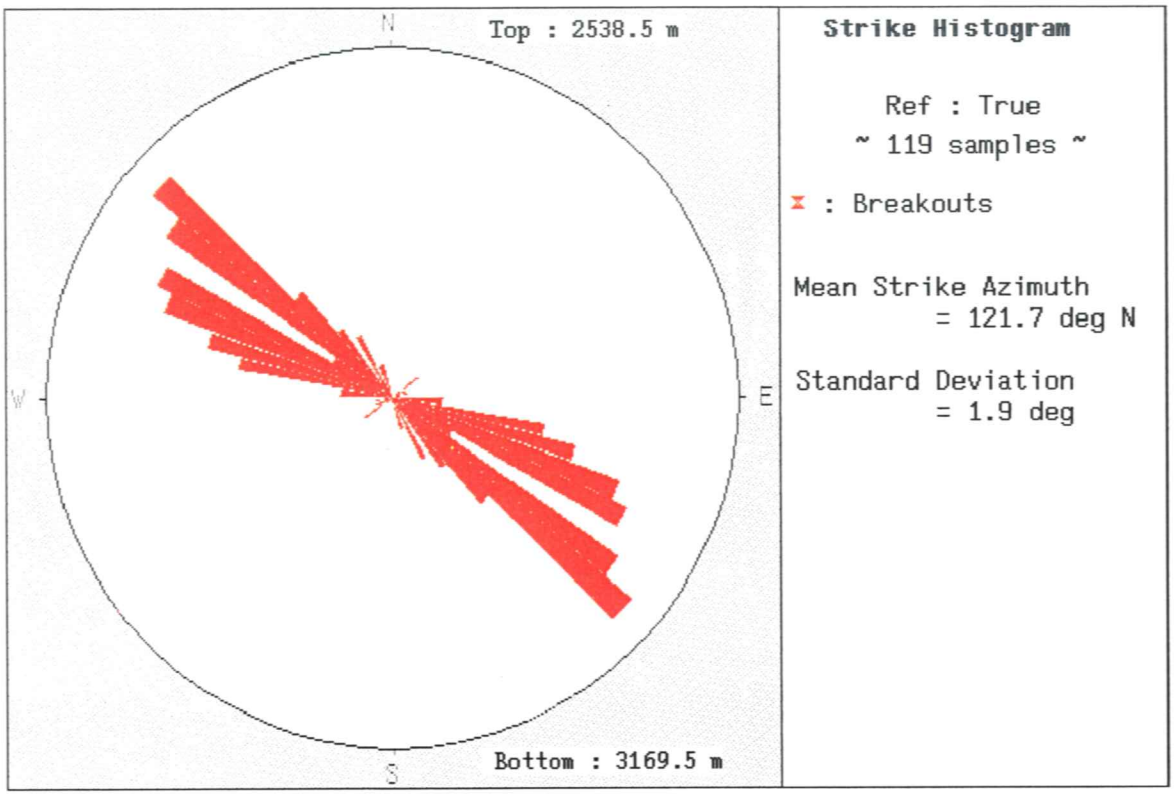
N
W
E
S
Top : 2538.5 m
Bottom : 3169.5 m
Strike Histogram
Ref : True
~ 119 samples ~
: Breakouts
Mean Strike Azimuth
= 121.7 deg N
Standard Deviation
= 1.9 deg

References

Aadnoy, B.S.
1990: In-situ stress directions from borehole fracture traces; in Journal of Petroleum Science and Engineering, vol. 4, p. 143-153.

Bell, J.S., Price, P. R., and McLellan P. J.
(accepted 1992): In-situ stress in the western Canada sedimentary basin; Geological Atlas of the Western Canada Sedimentary Basin, Mossop, G. D., (Editor), Canadian Society of Petroleum Geologists, 7 figs, 4 tables, 3 maps, 27 p.

Bourke, L., Delfiner, P., and Fett, T.
1989: Using Formation Microscanner images; in The Technical Review, v.37, no.1, p.16-40.

Dart, R.L., and Zoback, M.L.
1989: Wellbore breakout stress analysis within the central and eastern continental United States; in The Log Analyst, January-February, p.12-25.

Dickey, P. A.
1986: Petroleum Development Geology, 3rd ed.

Ekstrom, M.P., Dahan, C.A., Chen, M.Y., Lloyd, P.M., and Rossi, D.J.
1987: Formation imaging with microelectrical arrays; in The Log Analyst, May-June, p.294-306.

Heliot, D., Etchecopar, A., and Cheung, Ph.
1990: New developments in fracture characterization from logs; in Maury and Fourmaintraux (Eds), Rock at Great Depth, p.1471-1478.

Lehne, K.A. and Aadnoy, B.S.
1992: Quantitative analysis of stress regimes and fractures from logs and drilling records of a north sea chalk field; in The Log Analyst, July-August, p. 351-359.

Mardia, K.V.
1972: Statistics of directional data: probability and mathematical statistics; Academic Press, London and New York, 357 p.

Parker, D.L., and Hefferman, P.D.
1992: Methods of determining induced fracture orientation - Ferrier field application; in Journal of Canadian Well Logging Society, vol. 18, p.7-20.

Plumb, P.A., and Hickman, S. H.
1985: Stress-induced borehole elongation: a comparison between the Four-Armed Dipmeter and the Borehole Televiewer in the Auburn geothermal well; in Journal of Geophysical Research, vol.90, No.B7, p.5513-5521, June.

Plumb, R.A.
1989: Fracture patterns associated with incipient wellbore breakouts; in Maury and Fourmaintraux (Eds), Rock at Great Depth, p.761-768.

Prensky, S.
1992: Borehole breakouts and in-situ stress - a review; in The Log Analyst, May-June, p.304-312.

Zoback, M.D., Moos, D., and Mastin, L.
1985: Well bore breakouts and in situ stress; in Journal of Geophysical Research, vol. 90, no. B7, June 10, pp. 5523-5530.